ELSEVIER

Agricultural and Forest Meteorology 85 (1997) 117–132

AGRICULTURAL AND FOREST METEOROLOGY

Radiation absorption and use by humid savanna grassland: assessment using remote sensing and modelling

X. Le Roux [a,*], H. Gauthier [a], A. Bégué [b], H. Sinoquet [c]

[a] *Ecole Normale Supérieure, Laboratoire d'Ecologie (URA 258 CNRS), 46 rue d'Ulm, 75005 Paris, France*
[b] *Maison de la Télédétection (CIRAD-CA), 500 avenue J.F. Breton, 34093 Montpellier Cedex 05, France*
[c] *U.A. Bioclimatologie-PIAF (INRA-Université Blaise Pascal), Domaine de Crouelle, 63039 Clermont-Ferrand Cedex 02, France*

Received 11 March 1996; revised 10 December 1996; accepted 28 December 1996

Abstract

The components of the canopy radiation balance in photosynthetically active radiation (PAR), phytomass and leaf area index (LAI) were measured during a complete annual cycle in an annually burned African humid savanna. Directional reflectances measured by a hand-held radiometer were used to compute the canopy normalized difference vegetation index (NDVI). The fraction f_{APAR} of PAR absorbed by the canopy (APAR) and canopy reflectances were simulated by the scattering from arbitrarily inclined leaves (SAIL) and the radiation interception in row intercropping (RIRI) models.

The daily PAR to solar radiation ratio was linearly related to the daily fraction of diffuse solar radiation with an annual value around 0.47. The observed f_{APAR} was non-linearly related to NDVI. The SAIL model simulated reasonably well directional reflectances but noticeably overestimated f_{APAR} during most of the growing season. Comparison of simulations performed with the 1D and 3D versions of the RIRI model highlighted the weak influence of the heterogeneous structure of the canopy after fire and of the vertical distribution of dead and green leaves on total f_{APAR}. Daily f_{APAR} values simulated by the 3D-RIRI model were linearly related to and 9.8% higher than observed values.

For sufficient soil water availability, the net production efficiency ε_n of the savanna grass canopy was 1.92 and 1.28 g DM MJ^{-1} APAR (where DM stands for dry matter) during early regrowth and mature stage, respectively.

In conclusion, the linear relationship between NDVI and f_{APAR} used in most primary production models operating at large scales may slightly overestimate f_{APAR} by green leaves for the humid savanna biome. Moreover, the net production efficiency of humid savannas is close to or higher than values reported for the other major natural biomes. © 1997 Elsevier Science B.V.

1. Introduction

Estimating and modelling the structure and productivity of ecosystems has been widely prompted by attempts to understand ecosystem functioning at the local scale. Recently, it has understandably gained in interest with increasing awareness of the impact of large-scale phenomena such as global climate change and land-use changes. Net primary production models range from statistical models (e.g. Lieth, 1975) to process models taking into account photosynthetic assimilation, respiration and assimilate allocation (e.g. Coughenour et al., 1984). Attractive process

* Corresponding author at: U.A. Bioclimatologie-PIAF (INRA-Université Blaise Pascal), Domaine de Crouelle, 63039 Clermont-Ferrand Cedex 02, France. Tel: 33-4 73 62 43 33; fax: 33-4 73 62 44 54; e-mail: xleroux@clermont.inra.Fr.

0168-1923/97/$17.00
PII S0168-1923(97)00002-6

models can be linked to remotely sensed observations and thus show potential for assessing large-scale patterns in ecosystem production (Running et al., 1989). However, process models generally require numerous and specific measurements hardly attainable either over extensive regions or at the local scale. This implies that arbitrary values have to be used for some parameters or that these models have to be calibrated. Parametric models offer an alternative to simple statistical models and to sophisticated process models. An increasingly used parametric model to estimate primary production was proposed 2 decades ago by Monteith (1972). This author showed that phytomass production is strongly correlated with the amount of photosynthetically active radiation or PAR (400–700 nm) absorbed by plants (APAR). Monteith (1977) suggested a form of primary production model as the time integral:

$$P_n = \int_t \varepsilon_n f_{APAR} \varepsilon_s \boldsymbol{R}_s \mathrm{d}t \qquad (1)$$

where P_n is the net primary production (g m^{-2}), $\boldsymbol{R}_s$ is the total downward solar radiation (MJ m^{-2} day^{-1}), ε_s is the ratio of incident PAR to $\boldsymbol{R}_s$, f_{APAR} is the fractional absorption of PAR by the canopy, and ε_n (the net production efficiency) is the ratio of net primary production to absorbed PAR (g MJ^{-1} APAR).

This parametric model subsumes the physiognomic and physiological complexities of primary production processes into two variables: fractional absorption of PAR and net production efficiency. Thus, it is a tool in understanding vegetation growth but cannot be expected to serve as a single and universal account of plant production as recently discussed in a volume of this journal (Demetriades-Shah et al., 1994, Monteith, 1994, and others). To be generalized, this model has to be calibrated against direct measurements of light absorption and production in all conditions that it is to be applied to, which is tedious and time-consuming for small research plots. Such direct measurements would be prohibitive over large areas. Thus, efforts have been made to establish the applicability of the model at the large scale. This led to the following.

1. The development of relationships between f_{APAR} and spectral reflectances of canopies: As for other biophysical process rates in vegetation, the fraction of PAR absorbed by the canopy can be linked experimentally to reflectance data (Kumar and Monteith, 1981, Asrar et al., 1984, Hatfield et al., 1984, Gallo et al., 1985 among others). Theoretical analysis of radiative interactions in plant canopies (Choudhury, 1987, Sellers, 1987, Goward and Huemmrich, 1992) has subsequently corroborated these empirical results.
2. The explicitation of environmental effects (i.e. water, temperature, nutrients) on ε_n (Runyon et al., 1994, Prince and Goward, 1995): Evaluating the importance of these factors requires experimental studies at the ecosystem level.

Radiation absorption and conversion into net primary production have been studied essentially for temperate and tropical crops (for a review, see Prince, 1991). However, data concerning natural vegetation types are scarce (for a review, see Ruimy et al., 1994). To our knowledge, very few measurements were performed in non-forested natural tropical biomes. Studies were carried out in a mesic savanna in Kenya (Kinyamario and Imbamba, 1992), in a dry fallow savanna in Niger (Bégué et al., 1996, Hanan et al., 1997) and for Sahelian grasslands (Hanan et al., 1995). Hitherto, the only data available for humid tropical grasslands reported the net production efficiency based on total solar radiation intercepted by green plus dead matter in a monsoon grassland in Thailand (Kamnalrut and Evenson, 1992). This lack of data is dramatic since tropical grasslands cover 15×10^6 km^2, an area of the same order as the area covered by tropical forests (Lieth, 1975). Furthermore, ecological field studies have underlined the high net primary productivity of this biome (Long et al., 1989) and the importance of its influence on global carbon cycling (Hall, 1989). Therefore, understanding and modelling the seasonal variations of the fractional absorption of radiation and net production efficiency of these ecosystems is necessary before Monteith's model can be used to assess their role in local, regional or global carbon budgets.

The study presented here was part of an extended experimental programme dealing with savanna–atmosphere exchanges conducted from January 1991 to June 1994 (Le Roux, 1997a). This paper aims to determine Monteith's model parameters for the grass canopy in open areas of an *Hyparrhenia/Andropogon*-dominated humid savanna, one of the major

biomes in the humid tropics (*Hyparrhenia* and *Andropogon* sp. introduced from Africa often displace the native C_4 grasses from South American tropical savannas: see Fischer et al., 1994). Results acquired in shrubby areas will be presented in another paper. The objectives of this work were: (1) to quantify radiation absorption and net production efficiency throughout a whole annual cycle, (2) to explain variations of these parameters by changes of biological parameters (leaf area index, growth stage and water status), (3) to compare f_{APAR} values measured and simulated by two radiation transfer models (scattering from arbitrarily inclined leaves (SAIL) and 1D radiation interception in row intercropping (RIRI) models assuming that the canopy is homogeneous; and 3D-RIRI model representing the horizontal and vertical structures of the canopy) and (4) to compare the relationships between f_{APAR} and a spectral vegetation index provided by ground measurements or simulations. Implications for quantitative remote assessment of primary production in the humid savanna zone are discussed.

2. Materials and methods

2.1. Study site

The Guinea savanna domain is defined as a zone of dense and high grass layer with scattered trees where annual precipitation exceeds 1000 mm and the dry season is less than 2 months. In central West Africa, Guinea savannas extend north of the equatorial forests to 9°N and cover roughly 0.5×10^6 km^2. The study was carried out at the Lamto Reserve (6°13′N, 5°02′W), in a typical Guinea savanna of Ivory Coast (Menaut and César, 1979). At Lamto, annual precipitation is 1200 mm (1962–1993 period). Well-defined periods of precipitation occur: a long rainy season from March to November, usually interrupted by a short dry season in August, and a long dry season from December to February. Temperatures (annual mean 27.7°C) are quite constant throughout the year. Savanna fires occur each year during the long dry season, generally in January, and consume much of the grass layer. Grasses regrow quickly and the canopy is closed around 3 months after the fire occurrence.

The study was carried out in an open shrubby savanna combining large grassy areas and shrubby areas. This savanna type covers half of the Lamto area. A 60-m × 60-m grass plot was selected in order to measure continuously the radiation budget and biological properties of the vegetation during a 1-year period. The grass layer consisted mainly of C_4 grass species dominated by *Andropogon* sp. and *Hyparrhenia* sp.; *A. canaliculatus*, *A. schirensis*, and *H. diplandra* are the dominant grasses on the study site. A detailed ecological description of the study site can be found in Le Roux (1995).

2.2. Radiation measurements

2.2.1. Canopy radiation balance

During the first 3 months after fire, the grass canopy is sparse. To overcome the problem of sampling this canopy and to get hourly and daily measurements, a permanent array of a large number of sensors was deployed. The sensors used were amorphous silicon cells which include PAR (400–700 nm) and shortwave (400–1100 nm) detectors (Bégué et al., 1996).

Radiation measurements were made on a 10-m × 10-m plot within the 60-m × 60-m grass area (Gauthier, 1993). Two cells (2.5 m above ground level) measured incident radiation. Four downward-facing cells (2.5 m above ground level) measured radiation reflected by the canopy. Five sets of ten cells located at ground level measured transmitted radiation. Two downward-facing cells, 0.4 m above a plot where vegetation was removed, measured radiation reflected by bare soil surface. Global and diffuse solar radiation was measured at 2.5 m above ground level by two Kipp and Zonen pyranometers, one equipped with a shade ring. All radiation sensors were connected to a Campbell 21X data logger. Sample measurements at 10-s intervals provided 20-min average values during the diurnal period (5:40 to 19:20) from April 1993 to May 1994. Instrumentation was removed for 2 weeks in January at the time of fire occurrence.

Before the experiment in April 1993, in August 1993, after fire occurrence in January 1994 and after the experiment in May 1994, in situ calibrations were carried out between all the PAR detectors and a reference PAR quantum sensor (Pontailler, 1990)

calibrated against a LI-COR quantum sensor. Shortwave sensors were calibrated against a reference Kipp and Zonen pyranometer. As observed by Bégué et al. (1996), the PAR sensors were stable over time while the shortwave radiation sensors exhibited a non-negligible time variability (ca 8%) which was corrected. Near infrared radiation was calculated as the difference between total shortwave and PAR radiation.

The fractions of PAR intercepted (f_{IPAR}) or absorbed (f_{APAR}) by the canopy were calculated as:

$$f_{IPAR} = 1 - \tau \quad (2)$$

$$f_{APAR} = 1 - \rho - \tau + \tau\rho_s \quad (3)$$

where τ is the ratio between transmitted and incident radiation, and ρ and ρ_s are the hemispherical reflectances (i.e. spectral albedo) of the canopy and of the bare soil, respectively. Daily f_{IPAR} or f_{APAR} was calculated as the ratio between the daily intercepted or absorbed radiation and the daily incident radiation between sunrise and sunset. Measured f_{IPAR} or f_{APAR} values correspond to radiation intercepted or absorbed by green plus dead leaves.

2.2.2. Canopy spectral reflectances

Red (610–680 nm) and near infrared (790–890 nm) canopy reflectances were measured at ground level throughout the annual vegetation cycle with a CIMEL radiometer. The radiometer bands simulate the sensors on board SPOT (Satellite Probatoire d'Observation de la Terra) satellites. Measurements were carried out between 11.30 a.m. and 1.30 p.m. (i.e. solar elevation ranging from 65° to 85°) on clear days. The 12° field of view radiometer was mounted on a boom truck assembly 2.5 m above the soil surface and levelled for vertical viewing. Reflectances were measured on at least six plots of grass canopy and two plots of bare soil. Reflected radiation from a white barium sulphate reference panel was measured concurrently. Canopy reflectance factors were calculated as the ratio of the canopy to the reference panel radiances. Near infrared (ρ_{nir}) and red (ρ_r) canopy reflectance factors were used to compute the normalized difference vegetation index (NDVI):

$$NDVI = (\rho_{nir} - \rho_r)/(\rho_{nir} + \rho_r) \quad (4)$$

2.3. Biological measurements

2.3.1. Leaf area index and canopy structure

Phytomass was clipped at 4- or 2-week intervals in four open areas located close to the radiation plot. Two 4-m^2 quadrats were sampled at each location (i.e. 8×4 m^2 at each sampling date). Green and dead phytomasses were sorted and dried to constant weight at 80°C. The green and dead leaf areas were calculated using the seasonal variations of green and dead specific leaf areas determined for the same site by Le Roux (1995) during the 1992 vegetation cycle. Green and dead phytomass vertical distribution was measured at four stages during the growing season on four 1-m^2 plots (Gauthier, 1993). Leaf angle distribution was measured at three vegetation stages during the growing season. One hundred leaf angle measurements were performed for each 10-cm layer of the grass canopy (Gauthier, 1993). The fractional cover of the grass layer was assessed by the point contact method with measurements at 0.1-m intervals on four 10-m transects.

2.3.2. Root-to-shoot allocation after fire

Estimates of net production efficiency could be strongly biased if root-to-shoot allocation is not taken into account, particularly just after fire. Thus, a rough estimate of potential root-to-shoot allocation was obtained during the 45-day period following fire by comparing the in situ grass regrowth in darkness and on control plots. A randomized block design was used: six blocks of six quadrats were shaded by totally opaque plastic enclosures which were protected from direct radiation by insulating shelters located 50 cm above each enclosure; six unshaded blocks of six quadrats provided control plots. Changes in above-ground phytomass were measured at each of six dates by clipping one shaded and one control quadrat (1 m × 1 m) in each block. Three 41-cm^2 soil cores were removed from the centre of each quadrat to a depth of 60 cm. Root material was extracted by washing over a 0.5-mm-mesh sieve and dried to constant weight at 80°C. The shaded quadrats were watered to simulate the rainfall regime of control plots. Incident PAR in enclosures was always below the sensor detection limit (PAR < 5 μmol m^{-2} s^{-1}). Air temperature measured in enclosures

with Cu/Cst thermocouples was always less than 3°C higher than screen air temperature above control plots. Grasses died after 45 days on shaded plots but no dead matter was observed before.

2.3.3. Calculation of primary production and net production efficiency

Best estimates of above-ground net primary production (ANPP) of the Lamto savanna are obtained by summing the positive increments of biomass and necromass, and the quantity of necromass disappeared between two sampling dates (Fournier and Lamotte, 1983). A constant rate of necromass disappearance (0.015 day^{-1}) was chosen according to values estimated by Le Roux (1995). Just after fire, above-ground production was assumed to be equal to the difference between phytomass accumulation on control plots and on shaded plots. At the annual scale, total net primary production (TNPP) was assumed to be equal to two-fold ANPP as reported by Menaut and César (1979) for open shrubby savannas at Lamto.

The value of the net production efficiency, ε_n, is often calculated as the slope of the best-fit line on a plot of cumulative dry matter versus cumulative intercepted or absorbed PAR. This is not statistically justifiable (Russel et al., 1989, Demetriades-Shah et al., 1992), and ε_n is rarely constant along a vegetation cycle. Thus, ε_n was computed as the ratio between the finite net primary production and the finite amount of absorbed PAR between two sampling dates. Soil water status during the period studied was assessed by a water balance model validated at the same site (Le Roux, 1997b). At Lamto, grasses experience water stress when the ratio of actual to maximum available soil water contents in the 0–60-cm soil layer is below 0.4 (Le Roux, 1997b).

2.4. Radiation transfer models

2.4.1. The SAIL model

The SAIL model (scattering from arbitrarily inclined leaves; Verhoef, 1984) is an extension of the Kubelka–Munk theory of light scattering and extinction in diffusing media. Flux extinction and scattering coefficients of each vegetation layer are calculated on the basis of (1) leaf area index, (2) leaf inclination distribution and (3) optical properties of single leaves and parameters associated with measurement conditions (soil reflectance, fraction of diffuse radiation, sun and sensor angular position). The model assumes that the canopy consists of several uniform layers of an infinite horizontal dimension. The leaves are assumed to be small, spatially independent and with a uniform azimuth distribution. Diffuse flux is isotropic and leaves are treated as bi-Lambertian scatterers.

A version of the SAIL model with two layers was used. Green vegetation was assumed to overtop dead leaves. Simulations were performed eight times a diurnal cycle. Daily f_{APAR} was computed according to the observed diurnal cycle of the fraction of global and diffuse solar radiation.

2.4.2. The RIRI model

The 3D model used in this study is an extension of the previously described 2D RIRI model (radiation interception in row intercropping; Sinoquet and Bonhomme, 1992). The model is based on the turbid medium analogy. The canopy is treated as an array of 3D contiguous cells which contain foliage from either 0, 1 or several vegetation components (here green and dead leaf area). Each cell is characterized by the leaf area density and leaf angle distribution of each component. Exchanges between radiation sources (incident radiation from the sky and scattered radiation from leaf area and soil surface) and receivers (leaf area, soil surface and the sky for reflected radiation) are computed from the fate of directional beams sampled in the horizontal plane above the canopy. Beam interception within the cells is derived from Beer–Lambert's law adapted to account for light partitioning between components (Sinoquet and Bonhomme, 1991). Scattering treatment uses a simplified phase function which involves a single leaf scattering coefficient (i.e. which does not distinguish leaf reflectance and transmittance) and only depends on the exit direction. The radiation balance including multiple scattering is solved using an approach similar to the radiosity method (Ozisik, 1981). Unlike the SAIL model, the RIRI model applies to non-horizontally homogeneous canopies, allows for foliage mixing of several components at a given location, treats the incident

diffuse radiation as a set of directional sources and uses a rather simplified treatment for the phase function.

In a first run, vegetation was represented by two (green and dead) layers without mixing as for the SAIL model. In a second run, horizontal heterogeneity of the bunch grass vegetation and vertical distribution of green and dead leaves were taken into account.

Grass bunches were represented by parallepipeds. Their height, H, was equal to the measured canopy height. Basal area was computed in order to match the volume of a hemisphere of radius H, i.e. the shape which best fits the bunch volume in the field. Bunch density was calculated in order to match the measured fractional vegetation coverage. Parallepipeds were randomly allocated on ground area according to field observations (Le Provost, 1993). This procedure allowed to fit the leaf area density within the bunch envelope. When dead matter was present, each parallepiped was divided into five layers of equal height. Each layer contained a proportion of total green and total dead leaf areas according to the observed vertical distribution of green and dead matter. Specific leaf area was assumed to be constant with height.

2.4.3. Model parameters

Most of the model parameters (Table 1) were derived from measurements. Absorptance and transmittance by green leaves were measured for a dominant grass species at Lamto by Bony (1977). Absorptance and transmittance by dead leaves were reported for the grass *Panicum virgatum* (Walter-Shea et al., 1992). For each day, soil reflectance was computed as a function of the gravimetric moisture in the upper 2-cm soil layer (Le Roux, 1997a). This moisture was measured daily with five replicates during the 1-year period studied (Gauthier, 1993). Canopy directional reflectances in red and near infrared were simulated by the SAIL and RIRI models according to the conditions experienced during in situ measurements (solar elevation, fraction of diffuse solar radiation and measured surface soil moisture). The SAIL and RIRI models were used to simulate PAR absorbed by green plus dead leaves. Simulations performed by the 3D-RIRI model were used to partition PAR between green and dead foliages.

Table 1
Values and sources of the parameters and variables used to run the SAIL and RIRI models

Parameter	Value	Source
Soil reflectance in PAR	Soil moisture dependent	Le Roux (1997a)
Green leaf reflectance in PAR	0.12	Bony (1977) [a]
Green leaf transmittance in PAR	0.10	Bony (1977) [a]
Dead leaf reflectance in PAR	0.30	Walter-Shea et al. (1992) [b]
Dead leaf transmittance in PAR	0.35	Walter-Shea et al. (1992) [b]
Soil reflectance in red	Soil moisture dependent	Le Roux (1997a)
Soil reflectance in near IR	Soil moisture dependent	Le Roux (1997a)
Green leaf reflectance in red	0.10	Bony (1977) [a]
Green leaf transmittance in red	0.08	Bony (1977) [a]
Dead leaf reflectance in red	0.40	Walter-Shea et al. (1992) [b]
Dead leaf transmittance in red	0.48	Walter-Shea et al. (1992) [b]
Green leaf reflectance in near IR	0.43	Bony (1977) [a]
Green leaf transmittance in near IR	0.53	Bony (1977) [a]
Dead leaf reflectance in near IR	0.45	Walter-Shea et al. (1992) [b]
Dead leaf transmittance in near IR	0.50	Walter-Shea et al. (1992) [b]
Leaf inclination distribution	10° classes	Measured
Green and dead leaf area indices	Daily input	Measured
Diffuse fraction of solar radiation	20-min averaged input	Measured

[a] Values obtained for *Andropogon* sp. at Lamto.
[b] Values obtained for *Panicum virgatum* L. yellow leaf.

3. Results

3.1. PAR to solar radiation ratio

The annual mean value of the daily PAR to solar radiation ratio ε_s was 0.467. Maximum ε_s values (ca 0.5) were recorded during overcast days (i.e. for daily fraction of diffuse solar radiation around 0.8). A weak linear relationship was obtained between ε_s and the daily fraction of diffuse solar radiation R_d/R_s (Fig. 1):

$$\varepsilon_s = 0.433 + 0.071(R_d/R_s)$$
$$(P = 0.0001;\ r^2 = 0.193;\ n = 334) \qquad (5)$$

3.2. Phenology and fractional absorption of PAR

During the 1993 cycle, green leaf area index increased from 0 after fire to 4 in November (Fig. 2). Standing dead matter began to accumulate 3 months after the fire occurrence and maximum dead leaf area index (4.8) was reached at the end of the year. Dead phytomass mainly accumulated in the lower canopy layers, while green phytomass exhibited an exponential increase with canopy depth and was partly mixed with dead matter (Fig. 3). The canopy was markedly erectophile, with leaf angles ranging predominantly from 60° to 90° (Fig. 4).

The canopy PAR albedo was close to that of bare soil and thus remained around 0.10–0.12 without any clear seasonal trend (Fig. 5). The canopy NIR (Near Infra Red) albedo increased from ca 0.15 to 0.4 during the growing season (Fig. 5). This trend is explained by the high reflectance of leaves in NIR. The seasonal variations of the fractional interception or absorption of PAR was close to the leaf area index (LAI) variations (Fig. 5). During the regrowth, f_{APAR} and f_{IPAR} increased rapidly and reached maximum values at the end of the year. Despite the decrease in green LAI observed during the last month before fire (Fig. 2), no clear decrease of f_{APAR} and f_{IPAR} was observed at this time since these values corresponded to total radiation absorbed or intercepted by green plus dead leaves. During two periods (day number around 125 and 440), a transient decrease of f_{APAR} and f_{IPAR} was observed, probably due to water-limited conditions, ensuing leaf rolling and a decrease in green LAI as observed in the field.

Fractional interception was higher than fractional

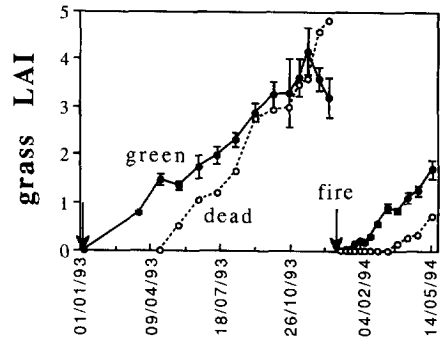

Fig. 2. Seasonal variation of the green and dead leaf area indices of the savanna grass canopy. Fire occurrences are indicated. Bars are standard errors.

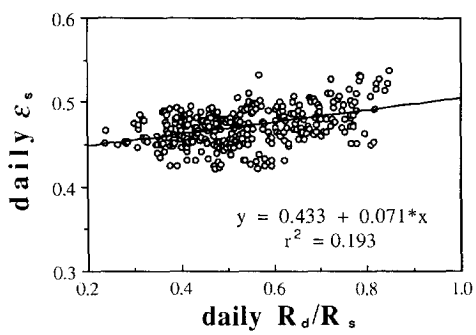

Fig. 1. Relationship between the daily PAR to solar radiation ratio ε_s and the daily fraction of diffuse solar radiation R_d/R_s. Values were obtained during the whole annual cycle. The linear regression line is plotted.

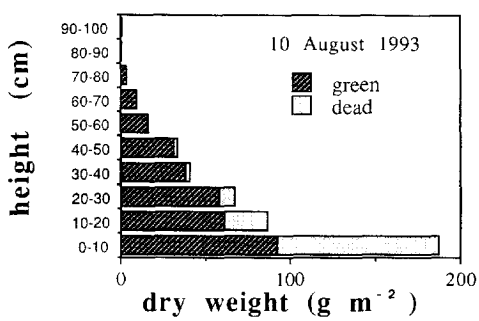

Fig. 3. Green and dead phytomass vertical distribution within the grass canopy. Measurements were performed on August 10, 1993.

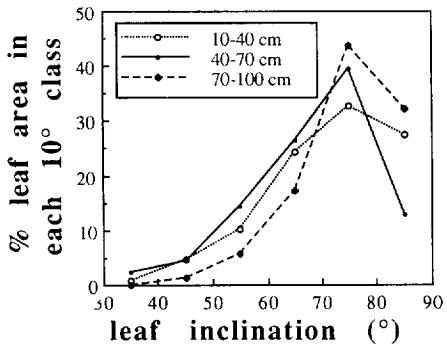

Fig. 4. Frequency distribution of leaf inclination (angle between the leaf normal and the vertical axis) in three different layers of the grass canopy (10–40 cm, 40–70 cm and 70–100 cm). Measurements were performed on August 10, 1993.

absorption (Fig. 5) since the former does not account for radiation reflected skyward by the canopy. Generally, f_{APAR} and f_{IPAR} are assumed to be very close because PAR absorptance by green leaves is very high. However, the difference between f_{APAR} and f_{IPAR} was not negligible ($f_{APAR} = 81\%$ and $f_{IPAR} = 92\%$) when the canopy was closed (Fig. 5).

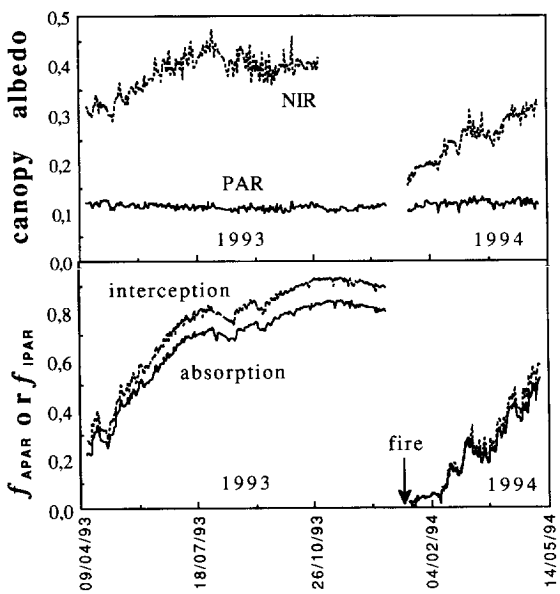

Fig. 5. Seasonal variation of (a) daily PAR and NIR canopy albedo, and (b) daily fractional interception and absorption of PAR by the savanna grass canopy. Fire occurrence is indicated.

3.3. Simulated versus observed f_{APAR} and reflectances

Both the SAIL model (Fig. 6) and RIRI model (not shown) were able to simulate red and near infrared directional reflectances reasonably well. In the red waveband, weak temporal variations were observed because of the similarity in the spectral response of the soil background and vegetation.

When the canopy is represented as two (green and dead) continuous vegetation layers without intermingling, the SAIL model noticeably overestimated the daily f_{APAR}, mainly for observed values ranging from 0.3 to 0.6 (Fig. 7). In the same conditions, the RIRI model provided better estimations for this range. Taking the horizontal structure of the bunch grass layer and vertical distribution of LAI into account slightly improved f_{APAR} estimates (Fig. 7). The daily f_{APAR} values simulated by the 3D-RIRI model were linearly related to the observed ones ($P = 0.0001$; $r^2 = 0.99$) and were systematically 9.8% higher than observed values. According to the 3D-RIRI model, PAR absorbed by green leaves ranged from 100% of total APAR for $f_{APAR} \leq 0.3$, to 79% of total APAR for $f_{APAR} = 0.8$. These values were used to compute PAR absorbed by green vegetation from the observed total f_{APAR}.

Partly due to the overestimation of f_{APAR} for intermediate f_{APAR} values, the SAIL model was unable to adequately simulate the relationship be-

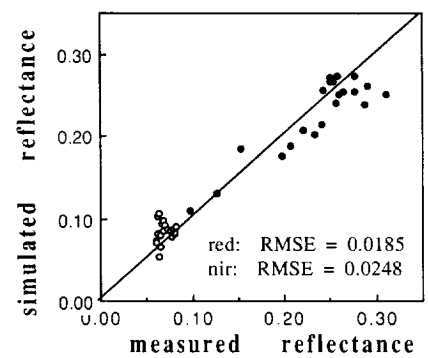

Fig. 6. Comparison of the red (○) and near infrared (●) directional reflectances measured in the field by the CIMEL radiometer and simulated by the SAIL model. The 1/1 line and the root mean square errors are indicated.

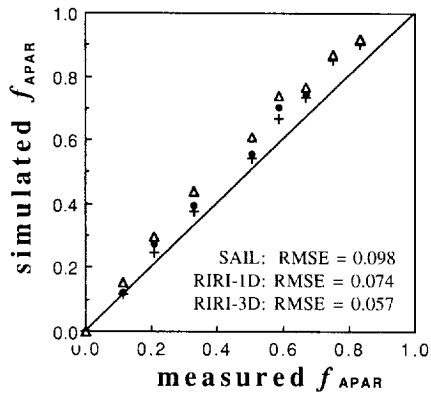

Fig. 7. Comparison of the daily fractional PAR absorption by green plus dead leaves f_{APAR} measured in the field and simulated. The SAIL model (△) and the 1D-RIRI model (●) assume that the canopy is horizontally homogeneous without overlapping between dead and green leaves. The 3D-RIRI model (+) accounts for the heterogeneous structure of bunch grasses and green and dead LAI vertical distribution. The 1/1 line and the root mean square errors are indicated.

tween f_{APAR} and the canopy NDVI (Fig. 8). When taking the canopy structure into account, the RIRI model provided a better, non-linear estimate of the relationship between total f_{APAR} and surface NDVI for this canopy (Fig. 8). However, both models do not provide a good representation of the field measurements: for a given NDVI, both models overestimate f_{APAR} which results in relatively large errors

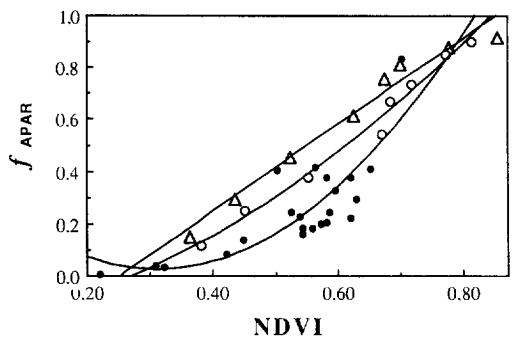

Fig. 8. Relationship between the daily total f_{APAR} and the canopy NDVI both observed in the field (●) or both simulated by either the SAIL model (△) or the 3D-RIRI model (○). The linear regression for SAIL simulations is $f_{APAR} = -0.653 + 2.17\,NDVI$ ($r^2 = 0.97$). The second order polynomial for RIRI simulations is $f_{APAR} = 0.182 - 1.618\,NDVI + 0.0378\,NDVI^2$ ($r^2 = 0.98$). The second order polynomial for observations is $f_{APAR} = 0.393 - 2.361\,NDVI + 3.782\,NDVI^2$ ($r^2 = 0.67$).

(RMSE = 0.182 and 0.098 for SAIL and 3D-RIRI, respectively). The 3D-RIRI model also provided a linear relationship between the fraction of PAR absorbed only by green leaves and NDVI:

$$f_{APAR-green} = -0.42 + 1.43\,NDVI$$
$$(P = 0.0001;\ r^2 = 0.99;\ n = 8) \quad (6)$$

3.4. Net production efficiency

During the first 40 days after fire, a significant above-ground dry matter accumulation was observed on shaded plots (Fig. 9). Maximum accumulation (12 g m^{-2}) was reached 1 month after the beginning of grass regrowth which occurred after the first rainfalls. This value was around 50% of the dry matter accumulated on control plots, which underlines the potentially high influence of root-to-shoot allocation on apparent above-ground production at this time. Concurrently, below-ground dry matter decreased from 1200 to 900 g m^{-2} with no significant differences between treatments (Fig. 9). This marked de-

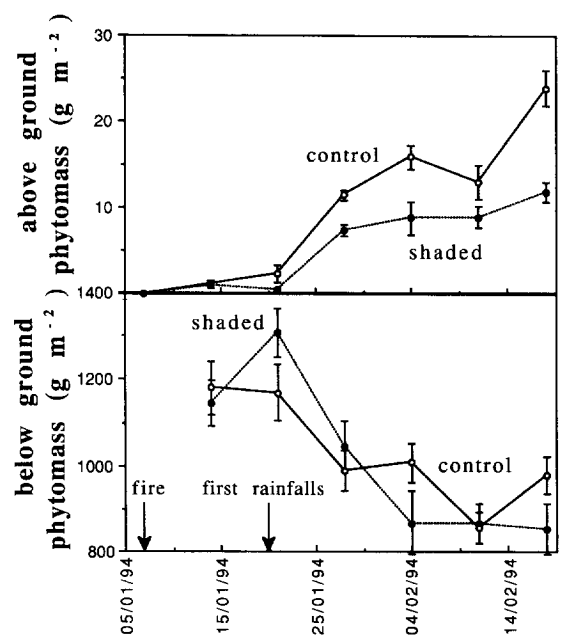

Fig. 9. Comparison of the variations in above-ground and below-ground phytomasses of the savanna grass canopy after fire in 1994 between control plots (○), and plots totally shaded (●). Bars are standard errors.

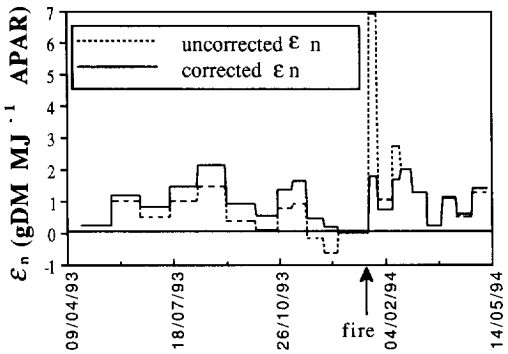

Fig. 10. Seasonal variations of the net production efficiency of the savanna grass canopy. Values are uncorrected (---) or corrected (————) to account for the disappearance of dead matter throughout the year, the estimated root-to-shoot allocation after fire occurrence and PAR absorption by dead matter.

crease could be due to the fast dead root decomposition at the beginning of the rainy season as observed during in vitro experiments (L. Abbadie, personal communication, 1996). Disappearance of standing dead matter accounted for 34% of the annual above-ground primary production (1290 g m^{-2} for the 1993 cycle).

Dead matter disappearance, root-to-shoot allocation after fire and radiation partitioning between green and dead leaves strongly influenced the calculation of net production efficiency (Fig. 10). Although regrowth can only be explained by root-to-shoot allocation on shaded plots where photosynthesis is excluded, shading can affect the microenvironmental conditions and the strength of source–sink relationships at the plant level. However, when this indirect index of root-to-shoot allocation was used to assess this process after fire, corrected values around 2 g DM MJ^{-1} APAR were more realistic than uncorrected ones (7 g DM MJ^{-1} APAR just after fire). The influence of correction for disappearance of dead matter was particularly high at the end of the annual cycle when standing dead matter is quantitatively important (uncorrected ε_n values were negative at the end of the cycle). Corrections applied to take the partitioning of APAR between dead and green leaves into account increased ε_n from 0 to 21% during the annual cycle.

The variability of ε_n through the year (Fig. 10) was explained by soil water availability and vegetation phenological stage (Table 2). With sufficient water availability, net production efficiency of absorbed PAR was higher during the early regrowth period than during mature stages.

4. Discussion

PAR is generally used as an important input variable in vegetation growth models. Accurate assessment of incident PAR is thus a prerequisite for these models. The annual value of the daily PAR to solar radiation ratio obtained at Lamto (0.467) is in agreement with values already reported for tropical regions (Stigter and Musabilha, 1982, Varlet-Grancher et al., 1982, Bégué, 1991, Bégué et al., 1996). Most growth models use a constant ε_s value since ε_s generally depends to a limited extent on atmospheric conditions (Varlet-Grancher et al., 1982). However, a weak but significant relationship between the daily ε_s and the daily fraction of diffuse solar radiation (i.e. essentially cloud cover at Lamto) was observed (Fig. 1). An increase of ε_s under

Table 2
Mean above-ground net production efficiency of absorbed PAR, ε_{na} (g DM MJ^{-1} APAR), or intercepted PAR, ε_{ni} (g DM MJ^{-1} IPAR), as a function of the vegetation phenological stage and soil water status and for the annual vegetation cycle. Root-to-shoot allocation after fire, disappearance of dead matter throughout the year and PAR absorption or interception by dead matter are taken into account. Standard errors are indicated in brackets

	ε_{na}	ε_{ni}	N
Early regrowth (LAI ≤ 0.6) no water stress	1.92 (0.09)	1.69 (0.11)	3
Early regrowth water stress	0.71 (–)	0.67 (–)	1
Mature stage (LAI > 0.6) no water stress	1.28 (0.13)	1.14 (0.11)	9
Mature stage water stress	0.60 (0.19)	0.54 (0.17)	7
Annual cycle	1.02 (0.14)	0.91 (0.12)	20

cloudy conditions was reported in tropical regions (Stigter and Musabilha, 1982). This is explained by the low cloud transmittance in the near-infrared region because high water vapour content are generally associated with high cloud cover. However, the uncertainty of ε_s values is of little importance compared with other difficulties (i.e. accurate estimation of f_{APAR} and ε_n) when Monteith's model is applied to assess savanna primary production in West Africa.

Both the SAIL and RIRI models overestimated total f_{APAR} for the Lamto grass canopy (Fig. 7). Two remarks can be made:

1. For intermediate f_{APAR} values, the SAIL model was found to provide higher f_{APAR} estimates than the 1D-RIRI model. This is consistent with results reported by Hanan et al. (1995) who observed that the SAIL model overestimated the daily interception efficiency of a sparse Sahelian canopy for f_{IPAR} higher than 0.3. The overestimation increased as f_{IPAR} increased from 0.3 to 0.5. The authors assumed that this overestimation could be due to a change in species composition through the season. Another explanation could be the choice of the distribution of incident diffuse radiation. The SAIL model uses an isotropic distribution (i.e. uniform overcast sky, UOC) while the RIRI model assumes a standard overcast sky (SOC) where radiance increases with elevation angle. SOC distribution leads to lower f_{APAR} since transmission of radiation coming from high elevations is high, especially in the case of erectophile foliage. This is confirmed since running the 1D-RIRI model with a UOC distribution provided f_{APAR} values very close to the SAIL outputs.
2. Taking the structure of the bunch grass layer and vertical distribution of LAI into account only slightly improved total f_{APAR} estimates (Fig. 7): RMSE = 0.074 and 0.057 for the 1D- and 3D-RIRI simulations, respectively. Thus, under the conditions encountered in this study, one-dimensional radiative transfer schemes designed for homogeneous canopies could be suitable for modelling total f_{APAR}. This result cannot be generalized since significant errors incurred in using a 1D model for simulating the radiation regime of steppe-like heterogeneous canopies were found by Asrar et al. (1992). In our study, the remaining discrepancy between observations and 3D-simulations (+9.8%) could be explained by errors in parameters used, LAI computation, representation of the canopy structure and/or radiation measurements.

The influence of the vertical distribution of green and dead leaves on the fraction of PAR absorbed by green leaves was significant. During the last 2 months, the fractional PAR absorption by non-photosynthetic material reached up to 21% (10% according to the 1D simulation). Thus, PAR absorption by dead leaves within the savanna grass layer should be considered in photosynthesis and growth estimates. This result applies for a few months in annually burned savannas, but all the year long in unburned savannas.

Both the SAIL and RIRI models simulated reasonably well directional reflectances. The RMSE values obtained (ca 2%, see Fig. 6) are similar to values reported by Hanan et al. (1995) who applied SAIL to Sahelian grasslands. However, reflectances are mostly underestimated in the NIR region while overestimated in the red waveband. A systematic underestimation of the NIR reflectance by the SAIL model was previously reported by Goel and Thompson (1984) for nadir viewing. Despite these small discrepancies, results obtained with the RIRI model may appear somewhat surprising because of the weak treatment of leaf scattering in this model. This good behaviour could be due to the very erectophile canopy (Fig. 4) where both reflection and transmission contribute to upward scattered radiation.

Nevertheless, the ability of both SAIL and RIRI models for simulating the relationship between f_{APAR} and NDVI is weak (Fig. 8). This may be partly due to a joint effect of: (i) overestimation of f_{APAR}; (ii) underestimation of NDVI resulting from the overestimation and underestimation of red and NIR reflectances, respectively. Although both model results are poor, the 3D-RIRI model simulations better match field measurements than the SAIL model ones (Fig. 8). Furthermore, differences between observed f_{APAR} and f_{APAR} inferred from the f_{APAR}–NDVI relationship provided by the RIRI model are significantly related to the soil surface humidity (linear model: $P = 0.014$, Fig. 11). This trend could be explained by differences in soil properties between the bare soil and vegetated plots, leading to different soil lines. Indeed, maintenance of bare plots may lead to

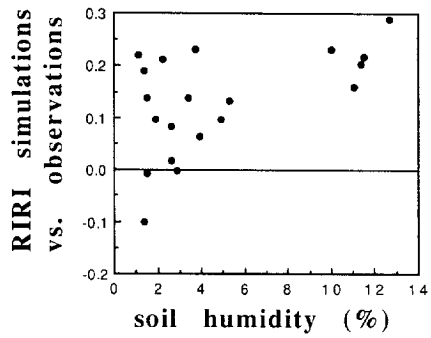

Fig. 11. Differences between the RIRI-3D f_{APAR} and observed f_{APAR} as a function of the humidity of the upper 0–2-cm soil layer. For each observed NDVI, the RIRI-3D f_{APAR} is estimated from the f_{APAR}–NDVI relationship simulated by RIRI-3D.

changes in soil surface colour and texture due to (i) increased leaching and runoff and (ii) absence of fire, especially in case of a 1-year-long experiment. Thus the soil darkness could be underestimated, which could markedly influence the f_{APAR}–NDVI relationship. Indeed, this relationship is seriously affected by the background spectral reflectance properties, and the curvilinearity of the relationship increases as soil reflectance decreases (Choudhury, 1987, Goward and Huemmrich, 1992). Ultimately, it is difficult to compare our findings to other studies since, to our knowledge, attempts to compare observed and modelled f_{APAR}–NDVI relationships are scarce. Authors generally report either fitted relationships between measured values of f_{APAR} and NDVI (e.g. Asrar et al., 1984, Hatfield et al., 1984, Walter-Shea et al., 1992), or f_{APAR}–NDVI relationships computed from simulation models without testing against field data (e.g. Asrar et al., 1992, Hanan et al., 1995).

The measured form of the NDVI relationship with total f_{APAR} was not linear, in contrast with results reported for wheat (Asrar et al., 1984, Hatfield et al., 1984), and tallgrass prairie (Walter-Shea et al., 1992) among others. However, a curvilinear relationship was obtained between f_{APAR} and NDVI for a corn canopy by Gallo et al. (1985). Choudhury (1987), Goward and Huemmrich (1992) and Bégué and Myneni (1996) pointed out that the form of this relationship depends on solar zenith angle, sensor view, canopy geometry, spectral characteristics of the leaves and moreover background spectral reflectance properties which strongly influence the curvilinearity of the f_{APAR}–NDVI relationship (Goward and Huemmrich, 1992). However, the practical significance of this result in remotely sensed APAR assessment is not fully documented. At Lamto, the soil is dark, particularly at the beginning of the vegetation cycle after fire occurrence. Using NOAA-AVHRR (National Oceanic and Atmospheric Administration; Advanced Very High Resolution Radiometer) data, Le Roux et al. (1994) showed that savanna fire induces low surface albedo observable at the regional scale in the Guinea savanna zone. In this context, a marked curvilinearity is expected between NDVI and f_{APAR}. The relevance of such non-linearity at large scales in the humid savanna zone has to be tested. Nevertheless, a linear relationship was observed between NDVI and fractional absorption by green leaves $f_{APAR-green}$, i.e. the relevant variable for detecting spatial and temporal variations of primary production using remotely sensed data.

For large-scale applications, the retained relationship between surface NDVI and f_{APAR} by green leaves assumes linear proportionality between f_{APAR} and NDVI, scaling the f_{APAR} estimates between zero at a minimum NDVI value representing soil background and a maximum value corresponding to the asymptotic maximum NDVI of a closed canopy. This method has been widely used in continental- or regional-scale applications of Monteith's production efficiency model (Ruimy et al., 1994, Runyon et al., 1994) or a modified version of this model (Maisongrande et al., 1995, Myneni et al., 1995). An alternative approach used by Hanan et al. (1995) for Sahelian vegetation canopies is to simulate the f_{APAR}–NDVI relationship with the SAIL model. Although our results do not bridge the gap between the understanding of small-scale processes and their representation at larger scales, they show that both these approaches could lead to inaccurate estimations of $f_{APAR-green}$ in grass-dominated West African humid savannas. On the one hand, the $f_{APAR-green}$–NDVI relationship provided by the SAIL model overestimated APAR by green leaves, essentially due to overestimation of total f_{APAR} and to an inadequate representation of the vertical structure of the canopy. On the other hand, a typical linear relationship scaling the f_{APAR} estimates between zero for soil NDVI and 0.9 for NDVI of a closed canopy (0.85) overesti-

mates APAR by green leaves when compared with Eq. (6). Thus, validation of f_{APAR}–NDVI relationships in all biomes, and assessment of the impact of PAR absorption by dead matter particularly for unburned savanna-like ecosystems, are warranted.

The accuracy and realism of the primary production values estimated by Monteith's model largely depend on an accurate estimation of the net production efficiency accounting for changes in environmental conditions. As pointed out by Gosse et al. (1986) and Russel et al. (1989), ε_n is rarely constant during a vegetation cycle and may vary with phenological stages or when environmental conditions are less favourable for growth. Prince (1991) suggested that the different factors that act on optimal ε_n values (no limiting factors) should be included in Monteith's model to account for environmental effects on this efficiency. Our data allow us to derive ε_n values in non-limiting water conditions for two phenological stages in the humid savanna studied (Table 2). In non-limiting water conditions, ε_n was higher during the early regrowth than during mature stages. This could be due to the relatively high nitrogen content exhibited by savanna grasses after fire and ensuing high photosynthetic rates as reported by Le Roux and Mordelet (1995).

ε_n was found to decrease during (1) drought periods during the growing season, and (2) senescence, although the last factor cannot be distinguished from the former because they act concurrently at the end of the year. The decrease in ε_n as the vegetation matures and senesces is well documented either for above-ground crop production (Ong and Monteith, 1985, Bégué, 1991) or total crop production (Gallagher and Biscoe, 1978, Green, 1987). The low efficiency at this time could be explained by (1) a decrease in new leaf production and the reduction of photosynthetic activity of the existing leaves with age, (2) an increase in respiration per unit of assimilation (Gallagher and Biscoe, 1978) and/or (3) changes in the partitioning of photosynthates. The decrease of ε_n observed at Lamto in limiting water conditions during the growing season should be explained either by an actual reduction of the primary production, or by an increase of the shoot-to-root allocation during drought periods, as reported for a lucerne crop by Durand et al. (1989).

The net production efficiency computed from above-ground production during the annual cycle studied is 1.02 g DM MJ^{-1} APAR. Thus, ε_n is 2.04 g DM MJ^{-1} APAR if total net primary production is assumed to be equal to two-fold the ANPP as reported by Menaut and César (1979) for open shrubby savannas at Lamto. As expected for nutrient-poor savannas which experienced periods of water shortage, the annual ε_n value is lower than typical values reported for fertilized and irrigated crops during the growing season (Table 3). However, ε_n values obtained for the Lamto grass canopy are as high as or higher than values reported for other major natural biomes (see the review by Ruimy et al., 1994). In

Table 3
Values of net production efficiency of absorbed or intercepted PAR (g DM MJ^{-1} APAR or IPAR) calculated for above-ground (A) or total (T) primary production in savanna ecosystems. Values reported by Kamnalrut and Evenson (1992) and by Kinyamario and Imbamba (1992), which correspond to net production efficiency of total solar radiation intercepted by green plus dead matter, are excluded. Values typical of C_4 and C_3 crops are presented for comparison

Vegetation	Country	Period	ε_n	Above-ground/total	Source
C_4 crop	–	Crop growing season	$\varepsilon_{na} = 2.5$	A	Gosse et al. (1986)
C_3 non-leguminous crop	–	Crop growing season	$\varepsilon_{na} = 1.9$	A	Gosse et al. (1986)
C_3 leguminous crop	–	Crop growing season	$\varepsilon_{na} = 1.7$	A	Gosse et al. (1986)
Sahelian savanna grass	Niger	70 days	$\varepsilon_{ni} = 0.79$	A	Hanan et al. (1995)
			$\varepsilon_{ni} = 2.21$	T	Hanan et al. (1995)
Humid savanna grass	Ivory Coast	1 year	$\varepsilon_{na} = 1.02$	A	This study
			$\varepsilon_{na} = 2.04$	T [a]	This study
Savannas (grass)	Continental production model		$\varepsilon_{na} = 2.39$	A	Loudjani (1993)
Savannas	Global production model		$\varepsilon_{na} = 1.26$	T	Ruimy et al. (1994)

[a] Assuming a below-ground/above-ground net primary productivity equal to unity (Menaut and César, 1979).

addition to relatively high ε_n, the long growing season of savanna grasses in the warm conditions of the tropics contributes to their high annual primary production.

Before this study, the net production efficiency of humid savannas was not documented, and data for dry savannas were scarce (Table 3). Thus, mostly inadequate values have been used for this biome in primary production modelling exercises performed at regional or global scales. The values of net production efficiency used by Loudjani (1993) and Ruimy et al. (1994) seem to be too high and too low, respectively (Table 3). On the one hand, Loudjani (1993) pointed out that erroneous ε_n values used in his study could explain the overestimation of estimated savanna primary production. On the other hand, low ε_n values of tropical forests and tropical grasslands could explain the low contribution of tropical latitudes to global NPP simulated by Ruimy et al. (1994). Two g DM MJ^{-1} APAR is a realistic value for the annual net production efficiency into total dry matter of West African savannas, although the effects of changing environmental conditions on ε_n are worth being made explicit. This value is equal to the upper limit of ε_n reported for old forest stands (Hunt, 1994).

5. Conclusion

The results presented here improve our understanding of the functioning of West African humid savanna-like ecosystems and have important implications for quantitative remote assessment of their primary production. These results highlight the fact that the relationship between NDVI and f_{APAR} used in most primary production models operating at large scales may be slightly inaccurate and has to be tested in this biome. Influence of PAR absorption by dead matter should be assessed. Our data also provide net production efficiency values in conditions of sufficient water availability or over the annual vegetation cycle which are useful to simulate humid savanna primary production at the local scale, and to validate models operating at larger scales. Taking into account the influence of the spatial variability of soil nutrient availability on ε_n remains a major challenge for remote assessment of primary production.

Acknowledgements

We express our gratitude to R. Vuattoux and J.L. Tireford, Directors of the Lamto Ecological and Geophysical Research Stations for all the facilities they offered us in the field. We thank E. Kouassi, F. N'Guessan and P. Savadogo for their technical assistance in the field, J.L. Rougean and L. Laguerre for help in preparing the experiment and A. Olioso for useful discussions. Grants from the SALT (SAvannas on the Long Term) Global Change and Terrestrial Ecosystems (GCTE)/International Geosphere Biosphere Programme (IGBP) core research project supported field data acquisition.

References

Asrar, G., Fuchs, M., Kanemasu, E.T., Hatfield, J.L., 1984. Estimating absorbed photosynthetic radiation and leaf area index from spectral reflectance in wheat. Agron. J. 76, 300–306.

Asrar, G., Myneni, R.B., Choudhury, B.J., 1992. Spatial heterogeneity in vegetation canopies and remote sensing of absorbed photosynthetically active radiation: a modeling study. Remote Sens. Env. 41, 85–103.

Bégué, A., 1991. Radiation use efficiency of pearl millet in the sahelian zone. Agric. For. Meteorol. 56, 93–110.

Bégué, A., Myneni, R.B., 1996. Operational relationships between NOAA-AVHRR vegetation indices and daily f_{APAR} established for Sahelian vegetation canopies. J. Geophys. Res. 101 D16: 21275–21289.

Bégué, A., Roujean, J.L., Hanan, N.P., Prince, S.D., Thawley, M., Huete, A., Tanré, D., 1996. Shortwave radiation budget of Sahelian vegetation during HAPEX-Sahel. 1. Techniques of measurement and results. Agric. For. Meteorol. 79: 79–96.

Bony, J.-P., 1977. Bilan radiatif du rayonnement solaire au dessus d'une savane de moyenne Côte d'Ivoire (Lamto). Bull. Liaison Cherch. Lamto IIs, 1–144.

Choudhury, B.J., 1987. Relationships between vegetation indices, radiation absorption, and net photosynthesis evaluated by a sensitivity analysis. Remote Sens. Env. 22, 209–233.

Coughenour, M.B., McNaughton, S.J., Wallace, L.L., 1984. Modelling primary production of perennial graminoids – uniting physiological processes and morphometric traits. Ecol. Modelling 23, 101–134.

Demetriades-Shah, T.H., Fuchs, M., Kanemasu, E.T., Flitcroft, I., 1992. A note of caution concerning the relationship between cumulated intercepted solar radiation and crop growth. Agric. For. Meteorol. 58, 193–207.

Demetriades-Shah, T.H., Fuchs, M., Kanemasu, E.T., Flitcroft, I.D., 1994. Further discussions on the relationship between cumulated intercepted radiation and crop growth. Agric. For. Meteorol. 68, 231–242.

Durand, J.-L., Lemaire, G., Gosse, G., Chartier, M., 1989. Analyse de la conversion de l'énergie solaire en matière sèche par un peuplement de luzerne (*Medicago sativa* L.) soumis à un stress hydrique. Agronomie 9, 599–607.

Fischer, M.J., Rao, I.M., Ayarza, M.A., Lascano, C.E., Sanz, J.I., Thomas, R.J., Vera, R.R., 1994. Carbon storage by introduced deep-rooted grasses in the south American savannas. Nature 371, 236–238.

Fournier, A., Lamotte, M., 1983. Estimation de la production primaire des milieux herbacés tropicaux. Ann. Univ. Abidjan (Sér. E) XVI, 7–38.

Gallagher, J.N., Biscoe, P.V., 1978. Radiation absorption, growth and yield of cereals. J. Agric. Sci. Camb. 91, 47–60.

Gallo, K.P., Daughtry, C.S.T., Bauer, M.E., 1985. Spectral estimation of absorbed photosynthetically active radiation in corn canopies. Remote Sens. Env. 17, 221–232.

Gauthier, H., 1993. Echanges radiatifs et production primaire dans une savane humide d'Afrique de l'Ouest (Lamto, Côte d'Ivoire). DESS Thesis, University Toulouse, 37 pp.

Goel, N.S., Thompson, R.L., 1984. Inversion of vegetation canopy reflectance models for estimating agronomic variables IV: total inversion of the SAIL model. Remote Sens. Env. 15, 237–253.

Gosse, G., Varlet-Grancher, C., Bonhomme, R., Chartier, M., Allirand, J.-M., Lemaire, G., 1986. Production maximale de matière sèche et rayonnement solaire intercepté par un couvert végétal. Agronomie 6, 47–56.

Goward, S.N., Huemmrich, K.F., 1992. Vegetation canopy PAR absorbance and the normalized difference vegetation index: an assessment using the SAIL model. Remote Sens. Env. 39, 119–140.

Green, C.F., 1987. Nitrogen nutrition and wheat growth in relation to absorbed solar radiation. Agric. For. Meteorol. 41, 207–248.

Hall, D.O., 1989. Carbon flows in the biosphere: present and future. J. Geolog. Soc. 146, 175–181.

Hanan, N.P., Prince, S.D., Bégué, A., 1995. Estimation of absorbed photosynthetically active radiation and vegetation net production efficiency using satellite data. Agric. For. Meteorol. 76, 259–276.

Hanan, N.P., Prince, S.D., Bégué, A., 1997. Modelling vegetation primary production during HAPEX-Sahel using production efficiency and canopy conductance model formulations. In: Goutorbe et al. (Eds.), HAPEX-Sahel, Elsevier, Amsterdam.

Hatfield, J.L., Asrar, G., Kanemasu, E.T., 1984. Intercepted photosynthetically active radiation estimated by spectral reflectance. Remote Sens. Env. 14, 65–75.

Hunt, E.R., 1994. Relationship between woody biomass and PAR conversion efficiency for estimating net primary production from NDVI. Int. J. Remote Sens. 15, 1725–1730.

Kamnalrut, A., Evenson, J.P., 1992. Monsoon grassland in Thailand. In: Long, S., Jones, M., Roberts, M., (Eds.), Primary Productivity of Grass Ecosystems of the Tropics and Subtropics. Chapman and Hall, London, pp. 100–126.

Kinyamario, J., Imbamba, S.K., 1992. Savanna at Nairobi National Park, Kenya. In: Long, S., Jones, M., Roberts, M. (Eds.), Primary Productivity of Grass Ecosystems of the Tropics and Sub-tropics. Chapman and Hall, London, pp. 25–69.

Kumar, M., Monteith, J.L., 1981. Remote sensing of crop growth. In: Smith, H. (Ed.), Plants and the Daylight Spectrum. Academic Press, London, pp. 133–144.

Le Provost, E., 1993. Structure et fonctionnement de la strate herbacée d'une savane humide (Lamto, Côte d'Ivoire). DEA Thesis, University Paris 11, 38 pp.

Le Roux, X., 1995. Study and modeling of water and energy exchanges in the soil–plant–atmosphere continuum in a humid savanna. Ph.D. Thesis, University Paris 6, 203 pp. (in French).

Le Roux, X., 1997a. Soil–plant–atmosphere exchanges. In: Menaut, J.-C., Abbadie, L., Lepage, M. (Eds.), Lamto: A Savanna Ecosystem. Ecological studies, Springer Verlag, New York (in press).

Le Roux, X., 1997b. Modelling the savanna radiation balance, water balance and primary production. In: Menaut, J.-C., Abbadie, L., Lepage, M. (Eds.), Lamto: A Savanna Ecosystem. Ecological studies, Springer Verlag, New York (in press).

Le Roux, X., Polcher, J., Dedieu, G., Menaut, J.-C., Monteny, B.A., 1994. Radiation exchanges above West African moist savannas: seasonal patterns and comparison with a GCM simulation. J. Geophys. Res. 99 (D12), 25857–25868.

Le Roux, X., Mordelet, P., 1995. Leaf and canopy CO_2 assimilation in a West African humid savanna during the early growing season. J. Trop. Ecol. 11 (4), 529–545.

Lieth, H., 1975. Modeling the primary productivity of the world. In: Lieth, H., Whittaker, R.H. (Eds.), Primary Productivity of the Biosphere. Springer Verlag, New York, pp. 237–263.

Long, S.P., Garcia Moya, E., Imbamba, S.K., Kamnalrut, A., Piedade, M.T.F., Scurlock, J.M.O., Shen, Y.K., Hall, D.O., 1989. Primary productivity of natural grass ecosystems of the tropics: a reappraisal. Plant Soil 115, 155–166.

Loudjani, P., 1993. Apport des données satellitaires en vue de l'estimation de la production primaire à l'échelle régionale: cas de l'Afrique de l'Ouest. Ph.D. Thesis, University Paris 11, 151 pp.

Maisongrande, P., Ruimy, A., Dedieu, G., Saugier, B., 1995. Monitoring seasonal and interannual variations of gross primary productivity, net primary productivity and net ecosystem productivity using a diagnostic model and remotely-sensed data. Tellus 47B, 178–190.

Menaut, J.-C., César, J., 1979. Structure and primary productivity of Lamto savannas, Ivory Coast. Ecology 60, 1197–1210.

Monteith, J.L., 1972. Solar radiation and productivity in tropical ecosystems. J. Appl. Ecol. 2, 747–766.

Monteith, J.L., 1977. Climate and the efficiency of crop production in Britain. Phil. Trans. R. Soc. Lond. 281, 277–294.

Monteith, J.L., 1994. Validity of the correlation between intercepted radiation and biomass. Agric. For. Meteorol. 68, 213–220.

Myneni, R.B., Los, S.O., Asrar, G., 1995. Potential gross primary productivity of terrestrial vegetation from 1982–1990. Geophys. Res. Lett. 22, 2617–2620.

Ong, C.K., Monteith, J.L., 1985. Response of pearl millet to light and temperature. Field Crop Res. 11, 141–160.

Ozisik, N.M., 1981. Radiative Transfer. Wiley Intersci., New York, 575 pp.

Pontailler, J.-Y., 1990. A cheap quantum sensor using a gallium arsenide photodiode. Funct. Ecol. 4, 591–596.

Prince, S.D., 1991. A model of regional primary production for

use with coarse resolution satellite data. Int. J. Remote Sens. 12, 1313–1330.

Prince, S.D., Goward, S.N., 1995. Global primary production: a remote sensing approach. J. Biogeogr. 22, 815–835.

Ruimy, A., Saugier, B., Dedieu, G., 1994. Methodology for the estimation of terrestrial net primary production from remotely sensed data. J. Geophys. Res. 99, 5263–5283.

Running, S.W., Nemani, R.R., Peterson, D.L., Band, L.E., Potts, D.F., Pierce, L.L., Spanner, M.A., 1989. Mapping regional forest evapotranspiration and photosynthesis by coupling satellite data with ecosystem simulation. Ecology 70, 1090–1101.

Runyon, J., Waring, R.H., Goward, S.N., Welles, J.M., 1994. Environmental limits on net primary production and light-use efficiency across the Oregon transect. Ecol. Appl. 4, 226–237.

Russel, G., Jarvis, P.G., Monteith, J.L., 1989. Absorption of radiation by canopies and stand growth. In: Russel, G., Marshall, B., Jarvis, P.G. (Eds.), Plant Canopies: Their Growth, Form and Function. Cambridge University Press, Cambridge, pp. 21–39.

Sellers, P.J., 1987. Canopy reflectance, photosynthesis, and transpiration. II. The role of biophysics in the linearity of their interdependence. Remote Sens. Env. 21, 143–183.

Sinoquet, H., Bonhomme, R., 1991. A theoretical analysis of radiation interception in a two species plant canopy. Math. Biosci. 105, 23–45.

Sinoquet, H., Bonhomme, R., 1992. Modeling radiative transfer in mixed and row intercropping systems. Agric. For. Meteorol. 62, 219–240.

Stigter, C.J., Musabilha, V.M.M., 1982. The conservative ratio of photosynthetically active to total radiation in the tropics. J. Appl. Ecol. 19, 853–858.

Varlet-Grancher, C., Bonhomme, R., Chartier, M., Artis, P., 1982. Efficience de la conversion de l'énergie solaire par un couvert végétal. Acta Oecol., Oecol. Plant. 3, 3–26.

Verhoef, W., 1984. Light scattering by leaf layers with application to canopy reflectance modeling: the SAIL model. Remote Sens. Env. 16, 125–141.

Walter-Shea, E.A., Blad, B.L., Hays, C.J., Mesarch, M.A., Deering, D.W., Middleton, E.M., 1992. Biophysical properties affecting vegetative canopy reflectance and absorbed photosynthetically active radiation at the FIFE site. J. Geophys. Res. 97, 18925–18934.